Dynamic Control of Interference Limited Underlay D2D Network

Yunus Sarikaya, Hazer Inaltekin, Tansu Alpcan and Jamie Evans

arXiv:1606.00534v1 [cs.NI] 2 Jun 2016

***Abstract*—Device-to-Device (D2D) communication appears as a key communication paradigm to realizing the vision of Internet of Things (IoT) into reality by supporting heterogeneous objects interconnection in a large scale network. These devices may be many types of objects with embedded intelligence and communication capabilities, e.g., smart phones, cars, or home appliances. The issue in in this type of communication is the interference to cellular communication caused by D2D communication. Thus, proper power control and resource allocation should be coordinated in D2D network to prevent excessive interference and drastic decrease in the throughput of the cellular system. In this paper, we consider the problem of cross-layer resource allocation in time-varying cellular wireless networks with D2D communication and incorporate average interference to cellular system as a quality-of-service constraint. Specifically, each D2D pair in the network injects packets to its queue, at rates chosen in order to maximize a global utility function, subject to network stability and interference constraints. The interference constraint enforces an arbitrarily low interference to the cellular system caused by D2D communication. We first obtain the stability region for the multiuser systems assuming that the nodes have full channel state information (CSI) of their neighbors. Then, we provide a joint flow control and scheduling scheme, which is proven to achieve a utility arbitrarily close to the maximum achievable utility. Finally, we address the consequences of practical implementation issue such as distributed scheduling by a designing algorithm, which is capable of taking advantage of diversity gain introduced by fading channels. We demonstrate the efficacy of our policies by numerical studies under various network conditions.**

I. Introduction

The explosive increase of user demands leads to emergence of new data intensive applications to accommodate this increasing demand of users. One of the examples are 4G cellular technologies (WiMAX and LTE-A), which have efficient physical and MAC layer performance, but are still lagging behind extremely fast-increasing users' data demand. Therefore, researches are seeking for new paradigm in the context of 5G technologies to increase the efficiency of wireless network.

While the conventional cellular architecture consists of connections from base stations to user equipment, 5G systems may well rely upon a two-tier architecture consisting of a macrocell tier for base station to device communication, and a second device tier for device to device (D2D) communications. Such architectures are a hybrid of conventional cellular and adhoc designs. D2D communication in cellular networks is defined as direct communication between two mobile users without traversing the access point (AP) or first tier network. Hence directly communicating with nearby wireless device can highly increase the efficiency of the network by reusing cellular spectrum resources. This concept not only improves the efficiency of spectrum usage, but also has a great potential for enhancing the network performance expressed in terms of capacity, coverage, energy efficiency and end-to-end delays [1], [2]. For the above benefits, D2D communication is one of such technologies that appears to be a promising component in next generation cellular network.

In the literature, various paradigms are introduced based on the spectrum in which D2D communication occurs. These paradigms are classified as overlay and underlay inband and outband communications. The paradigm of interest in this paper is underlay inband communications, in which both D2D and cellular devices use the same spectrum to transmit their data. Operating in the same licensed band, devices will inevitably impact macrocell users by causing interference. To ensure minimal impact on the performance of existing APs, a two-tier network needs to be designed with smart interference management strategies and appropriate resource allocation schemes. Furthermore, users in today's cellular networks use real-time high data rate services like video sharing, gaming or proximity-aware social network. Those applications require end-to-end delay of incoming packets to be finite. Hence, the stability of user queues, i.e., the network stability, guaranteeing the delay to be finite, is another important design parameter, which should be taken into account.

Considering those design parameters, we combine a variety of basic networking mechanisms such as flow control and scheduling in the context of D2D underlaying cellular network. For that purpose, we model the entire problem as that of a network utility maximization, in which interference caused by D2D pairs to cellular BS is incorporated as an additional constraint and develop the associated dynamic flow control, power control, and scheduling mechanisms.

Scheduling in wireless networks is a prominent and challenging problem that attracted significant interest from the networking community. The challenge arises from the fact that the capacity of wireless channel is time-varying nature of wireless channels. Optimal scheduling in wireless networks has been extensively studied in the literature under various assumptions [3], [4], [5], [6]. Starting with the seminal work of Tassiulas and Ephremides [3], where throughput optimality of back-pressure algorithm is proven, policies opportunistically exploiting the time-varying nature of the wireless channel to

Y. Sarikaya, J. Evans ({yunus.sarikaya, jamie.evans}@monash.edu) and T. Alpcan (tansu.alpcan@unimelb.edu.au) are with the Department of Electrical and Computer Systems Engineering at Monash University, Australia

H. Inaltekin (hazeri@antalya.edu.tr) is with the Department of Electronics Engineering, Antalya International University, Turkey.

schedule users are shown to be at least as good as static policies [4]. In principle, these opportunistic policies schedule the user with the favorable channel condition to increase the overall performance of the system. However, without imposing individual performance guarantees for each user in the system, this type of scheduling may result in unfair sharing of resources and may lead to starvation of some users, for example, those far away from the base station in a cellular network. Hence, in order to address fairness issues, scheduling problem was investigated jointly with the network utility maximization problem [7], [8], and the stochastic network optimization framework that guarantees the network stability and provides fairness, was developed [9].

In our model, we consider a D2D network in which communication takes place regardless of cellular system as long as the interference caused by them to AP is kept low to guarantee a required level of Quality-of-Service (QoS) on the cellular network. We call such network *interference-aware* D2D network, In such setting, we use stochastic optimization framework to address the basic wireless network control problem in order to develop a cross-layer resource allocation solution that will incorporate interference metric to the AP as a QoS metric. Our main contributions are summarized as follows:

- **(a)** We evaluate the *stability region* of interference-aware D2D network, defined as the set of rates achievable by any flow control and link-scheduling scheme. Then, we compare it with the stability region where there is no interference constraint, and quantify the rate loss due to interference-aware operation of D2D network.
- **(b)** We formulate the resource allocation problem in interference-aware D2D network as a network utility maximization (NUM) problem, in which the optimal scheduling of D2D communication links allocation is implemented in the physical layer, while the flow control is realized in the transport layer.
- **(c)** Although there is no standard for D2D communications, D2D communications in cellular network are expected to be overseen/controlled by a central entity like evolved Node N (eNB). Thus, our first focus is to design a centralized algorithm. We propose a dynamic control algorithm, which is a joint scheduling and flow control scheme as the solution of the NUM problem, and we prove that this scheme achieves a utility arbitrarily close to the maximum achievable utility. Note that flow control algorithm moves the rate vector to the pareto boundary of the stability region based on defined utilities for the users. For example, logarithmic utility function moves the rates to the point where proportional fairness is satisfied.
- **(d)** We investigate important practical limitation, which is the unavailability of a centralized scheduler. Hence, we design a distributed scheduling algorithm called *channel-aware* distributed scheduler, where the devices decide to transmit or not based on their local information (i.e., based on their channel conditions and queue backlogs), and the proposed algorithm is channel-aware in the sense that they have capability of taking into account wireless channel variations. Then, we obtain performance bounds on the algorithms since the optimality can no longer be guaranteed due to availability of limited information. advantage of diversity gain imposed by fading channels. Then, we obtain performance bounds on the algorithms since the optimality can no longer be guaranteed due to availability of limited information.
- **(e)** We demonstrate via simulations the performance of proposed algorithms comparing with other well-known distributed schedulers and verify the analytical results.

II. Related Works

Our results in this paper are related to optimization in D2D communication in underlaying cellular network. Hence, we will only mention the papers which are most relevant to ours.

The authors of [10] and [11] consider a single cell scenario where a cellular user and two D2D users share the same spectrum, where the BS controls the transmit power and spectrum of the D2D communication link. The objective is to optimize the sum rate with energy/power constraint under non-orthogonal and orthogonal sharing mode. The authors show analytically that an optimal solution can be given either in closed form or can be chosen from a set. Then, the researchers turn their eyes on the efficient resource allocation with multiple D2D pairs. The work in [12] controls the interference of the D2D links to the cellular users by limiting the maximum transmit power of the D2D users. In [13], authors employ the interference-limited area knowledge for D2D receivers to maximize the network capacity with multiuser MIMO, and any cellular users in the vicinity of the interference-limited area is not scheduled. The optimal power allocation problem for D2D communication pairs are analyzed in [14], [15], [16], [17]. The authors in [14] and [16] showed that the problem of optimal power allocation and mode selection problem are rather involved and they propose heuristic approaches to solve the problem. The authors of [15] propose a method which applies exhaustive search to find power efficiency, which is a function of transmission rate and power consumption of the users.

The works in [18], [19], [20], [21], [22] focus on the improving the system performance while maintaining certain QoS constraint. The authors in [18] consider a resource allocation problem to maximize the overall network throughput while guaranteeing QoS requirements for both D2D and regular users. A maximum weight bi partite matching based scheme is developed to select a suitable D2D communication pair. [19] propose a graph-based resource allocation method, where they formulate the optimal resource allocation as a non-linear problem. Since the problem is NP-hard, they propose a suboptimal graph-based approach, which accounts for interference and capacity of the network. In their proposed graph, each vertex represents a link (D2D or cellular) and each edge connecting two vertices shows the potential interference the two links. [20] formulate the problem of maximizing the system throughput with minimum data rate requirements, and they use the particle swarm optimization framework to obtain the solution. In [22], the formulate the problem as integer

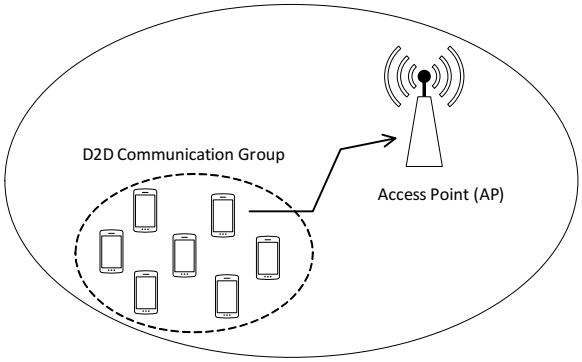

Fig. 1. Network model consisting of N D2D pairs that share a common frequency band with an access point.

programming problem. which is hard to solve due to being NP-hard. Hence, they propose a sub-optimal solution which is based on obtaining the elements of optimization problem in different phases.

On the other hand, the problems when the cellular infrastructure is missing, i.e., distributed algorithms where D2D users act autonomously, are mostly analyzed in a game-theoretical framework. In [23], the proposed approach optimally selects the most beneficial source devices by analyzing the interactions between the base station's rewarding strategies and the devices' transmission power using a Stackelberg game model. In addition to pricing model, [24] propose auction-based game theoretic models, where D2D communication pairs should bid for the channel to transmit their information. Other approaches propose a coalition formation game based scheme [25], [26], where cellular users and D2D communications pairs who want to communicate in the same spectrum, form a coalition. Most game-theoretical solutions impose large overhead due to the need for heavy information exchange in terms of bids, or prices and demands.

The solutions of these approaches and their derived sub-optimal heuristic can indeed improve the system performance with QoS constraints. However, they do not seem to be a good candidate for time-stringent application with limited computational capacity. Nonetheless, the authors of [10] and [11] derived the closed-form solution, which reduces the complexity. But they only consider a scenario with a cellular user and D2D communication pair, which is not practical in reality. The algorithm derived in this paper, which is shown to be close to optimal solution, is a simple index policy, i.e., the centralized entity performs simple algebraic manipulations to obtain the solution in each time instant. Furthermore, we consider a general network model which contains arbitraty number of D2D communication pairs.

III. System Model, Scheduling Policy and D2D Network Stability

In this section, we will introduce the details of our system model and the definitions of the main concepts that are used throughout the paper in relation to this model.

A. System Model

Our primary aim in this paper is to characterize the maximum rates of communication that can be *stably* supported by a D2D network and to discover the cross-layer *centralized* and/or *distributed* control mechanisms (i.e., flow control and scheduling) that can achieve these rates with provable performance guarantees. To this end, we consider a group of communication devices forming N distinct D2D communication pairs and sharing the same frequency band with an access point (AP), as shown in Fig. 1. The devices are in close proximity of each other so that they can reach to their intended receivers in a single hop, but they also cause excessive interference to each other when two or more pairs are active at the same time. This leads to a fully connected interference graph topology with collision model for the D2D network in question.

The devices operate in slotted time with slot indices represented by $t \in \mathbb{N}$. The link quality between the device pairs varies over time according to the *block* fading model, in which the channel gain is constant over a time slot and changes from one slot to another independently according to a common fading distribution. We use $h_i(t)$, $i = 1,\ldots,N$, to represent the *direct* channel gain between the transmitter and receiver of the ith D2D pair. These direct channel gains are independent and identically distributed (iid) over users as well as over time. Operating in the same frequency band, the devices also cause interference to the AP in Fig. 1, and we denote the *interference* channel gain between the transmitter of the ith D2D pair and the AP by $g_i(t)$, $i = 1,\ldots,N$. Again, interference channel gains obey to the iid block fading model (possibly with a different distribution than that of the direct channel gains) as described above. For notational simplicity, we often use the vector notation $\boldsymbol{h}(t) = [h_1(t),\ldots,h_N(t)]$ and $\boldsymbol{g}(t) = [g_1(t),\ldots,g_N(t)]$ to denote the channel gains more compactly.

For the sake of comprehending the interplay between the scheduling decisions at the MAC layer and the flow control decisions at the transport layer better, it is assumed that no power control is exercised at the physical layer of the D2D network and all devices transmit at a constant power level P over all time slots. This assumption will help us to distill the effect of physical layer parameters on the interactions of the upper layer scheduling and flow control protocols, which is the main focus of the current paper. In this setting, an important quantity of interest that determines the D2D network performance is the rates (measured in units of bits/slot) offered over a communication link during time slot t. We assume that these communication rates are described by the functions $R_i(t)$ (as functions of transmission power levels and channel gains) for $i = 1,\ldots,N$. Even though we do not assume any specific functional form for $R_i(t)$, which is usually determined by the coding and communication technologies embedded in the transceiver circuits of the devices,[1] we require that $R_i(t)$ has a bounded second moment, i.e., $\mathbb{E}\left[R_i(t)^2\right] \leq R_{max}^2$ for all

[1]For example, if the Shannon capacity formula is used to quantify the communication rates for the ith D2D pair, $R_i(t)$ can be given as $R_i(t) = \log\left(1+\frac{Ph_i(t)}{N_0}\right)$, where N_0 represents the total noise plus interference power degrading transmissions over the ith link. Indeed, these communication rates are achievable by using Gaussian codebooks when slot durations are large enough [27].

$t \in \mathbb{N}$. The significance of the rate function $R_i(t)$ in our analysis is that it will determine the *service* rates of the network layer queues maintained at the devices.

An application runs at the application layer of each device, and generates the bits to be stored at the transport layer queues of the devices. These bits are accepted to the network layer according to a *flow control* mechanism that runs at the transport layer. We let $A_i(t)$ represent the amount of data (in bits per slot) that enters the network layer at the beginning of time slot t and is stored at a network layer queue with size $Q_i(t)$ at device i. The relationship between these important network parameters at the queue level is displayed in Fig. 2.

It is assumed that the input rate $A_i(t)$ is admissible in the sense that $A_i(t) \leq A_{max}$ for all t, and it has a long-term average x_i, i.e., $x_i = \limsup_{T\to\infty} \frac{1}{T}\sum_{t=1}^{T} A_i(t)$. The utility obtained by the ith D2D pair $U_i(x_i)$ is a function of the long-term average rate x_i. We assume that $U_i(0) = 0$, and $U_i(\cdot)$ is a continuously differentiable, monotonically increasing and concave function of its argument. This concludes the description of our system model. In the next subsections, we will formally introduce the notions of scheduling policy and network stability as well as providing some main definitions classifying/characterizing the scheduling policies and the network stability region.

B. Scheduling Policy

Due to close geographical proximity of devices in our network model, only one D2D pair can communicate its data reliably over its respective wireless communication link. Hence, a scheduling decision must be made at the beginning of each time slot to select an *appropriate* user based on the current (both direct and interference) channel conditions. For this purpose, roughly speaking, a scheduling policy should determine which set of links to be activated in each time slot for data transmission.

Definition 1: A scheduling policy $\boldsymbol{\mathscr{I}} : \mathbb{R}_{+}^{2N} \mapsto [0,1]^N$ is a vector-valued function $\boldsymbol{\mathscr{I}}(\boldsymbol{h}(t),\boldsymbol{g}(t)) = [\mathscr{I}_1(\boldsymbol{h}(t),\boldsymbol{g}(t)),\ldots,\mathscr{I}_N(\boldsymbol{h}(t),\boldsymbol{g}(t))]^{\mathsf{T}}$ mapping the direct and interference channel states to scheduling probabilities, i.e., $\mathscr{I}_i(\boldsymbol{h}(t),\boldsymbol{g}(t)) \in [0,1]^N$ for $i \in \{1,\ldots,N\}$, for devices and satisfying the feasibility constraint $\sum_{i=1}^{N} \mathscr{I}_i(\boldsymbol{h}(t),\boldsymbol{g}(t)) \leq 1$.

It should be noted that scheduling policies given in Definition 1 constitute a collection of *randomized* control mechanisms for the D2D network in question specifying scheduling probabilities for each pair of device. Implicit in this definition, a scheduling policy does not allow two D2D pairs to be active simultaneously due to the topological constraints of our network model. More explicitly, once scheduling probabilities are identified for all D2D pairs for time slot t, *only one* of them is selected for transmission by using the probability distribution (possibly a defective one) induced by $\boldsymbol{\mathscr{I}}(\boldsymbol{h}(t),\boldsymbol{g}(t))$ over the set of device indices to determine the index of the selected D2D pair.

An important subset of the randomized scheduling policies introduced above is the deterministic ones. We say that a scheduling policy $\boldsymbol{\mathscr{I}}(\boldsymbol{h}(t),\boldsymbol{g}(t)) = [\mathscr{I}_1(\boldsymbol{h}(t),\boldsymbol{g}(t)),\ldots,\mathscr{I}_N(\boldsymbol{h}(t),\boldsymbol{g}(t))]^{\mathsf{T}}$ is a *deterministic* scheduling policy if $\mathscr{I}_i(\boldsymbol{h}(t),\boldsymbol{g}(t))$ is either zero or one for all $i \in \{1,\ldots,N\}$ and for all time slots t. It will be shown below that the use of randomized scheduling policies will facilitate the mathematical analysis of the collection of optimization problems leading to the network stability region by turning them into convex optimization problems, *whilst* the solutions of these optimization problems lie in the set of deterministic scheduling policies.

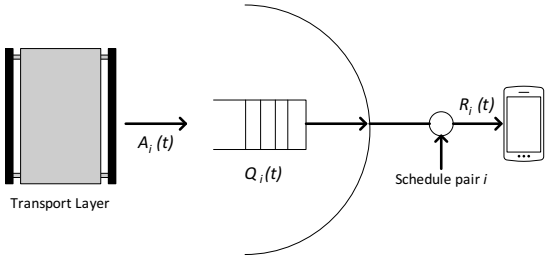

Fig. 2. Queue model of pair i.

C. D2D Network Stability

In this part, we will provide the details of the notion of the D2D network stability by relating the scheduling policies to the queue level dynamics of the devices. To this end, we will first put forward the notion of interference-aware D2D operation. All the network stability definitions presented afterwards will be with respect to the interference-aware D2D operation.

The main communication paradigm of interest that we focus on in this paper for the coexistence of a D2D network with an AP in the same spectrum is the *underlay* paradigm [28]. The main idea underpinning the underlay communication paradigm is that the D2D network can utilize the same spectrum with the AP as long as they do not cause harmful degradation to the data communication at the AP by keeping the interference levels (peak and average) below pre-specified interference threshold values. This leads to the interference-aware D2D operation, formally defined as below.

Definition 2: A D2D network is said to be an *interference-aware* D2D network if the average and peak interference power levels that it causes to the AP is bounded above by the pre-specified interference threshold values as

$$\sum_{i=1}^{N} \mathbb{E}_{\boldsymbol{h}(t),\boldsymbol{g}(t)}\left[P g_i(t) \mathscr{I}_i((\boldsymbol{h}(t),\boldsymbol{g}(t))\right] \leq \gamma \tag{1}$$

$$\sum_{i=1}^{N} P g_i(t) \mathscr{I}_i(\boldsymbol{h}(t),\boldsymbol{g}(t)) \leq \nu, \tag{2}$$

where γ and ν denote the upper limits on the *aggregate* average and instantaneous interference powers from all D2D links, respectively.

This definition makes the coupling between the scheduling policies and the restrictions due to the interference-aware operation of the D2D network explicit. In particular, the optimum scheduling policy achieving the maximum communication rates that can be stably supported by an interference-aware D2D network must strike a balance between choosing the best D2D link for device communication and respecting the radio etiquette rules arbitrating the spectrum access rights between

devices and the AP. The above interference constraints are primarily designed to safeguard two types of data traffic at the AP against the harmful D2D interference. The average interference constraint in (1) is for delay-insensitive data traffic (e.g., text messaging) for which the messages are encoded and decoded over many slots. On the other hand, the instantaneous interference constraint in (2) is for delay-sensitive data traffic (e.g., video streaming) for which the messages are encoded and decoded over a single time slot. A D2D network may not know the type of data traffic at the AP at any given particular time, and hence must respect both constraints simultaneously.

Next, we formally define the concept of the stability of an interference-aware D2D network. As is standard [9], stability here refers to being long-term averages of expected queue sizes finite, i.e., $\limsup_{T\to\infty}\frac{1}{T}\sum_{t=0}^{T-1}\mathbb{E}\left[Q_i(t)\right]<\infty$. Further, we say that the D2D network is stable under $\mathscr{I}\left(\boldsymbol{h}(t),\boldsymbol{g}(t)\right)$ if the network layer queues of all devices are stable. An important concept that expands upon definition of network stability and relates the flow control and scheduling mechanisms for a D2D network is the network stability region, which is defined as below.

Definition 3: The *network stability region* of an interference-aware D2D network, denoted by Λ, consists of all arrival rate vectors $\boldsymbol{x}=(x_1,x_2,\ldots,x_N)^{\intercal}$ such that there exists a scheduling policy $\mathscr{I}\left(\boldsymbol{h}(t),\boldsymbol{g}(t)\right)$ satisfying the conditions below for all $i\in\{1,\ldots,N\}$.

$$\mathbb{E}_{\boldsymbol{h}(t),\boldsymbol{g}(t)}\left[\mathscr{I}_i(\boldsymbol{h}(t),\boldsymbol{g}(t))R_i(t)\right]\geq x_i, \tag{3}$$

$$\sum_{i=1}^{N}\mathbb{E}_{\boldsymbol{h}(t),\boldsymbol{g}(t)}\left[Pg_i(t)\mathscr{I}_i(\boldsymbol{h}(t),\boldsymbol{g}(t))\right]\leq\gamma, \tag{4}$$

$$\sum_{i=1}^{N}Pg_i(t)\mathscr{I}_i((\boldsymbol{h}(t),\boldsymbol{g}(t))\leq\nu,\ \text{and}\ \sum_{i=1}^{N}\mathscr{I}_i((\boldsymbol{h}(t),\boldsymbol{g}(t))\leq 1. \tag{5}$$

The constraints in (4) and (5), they are due to the interference-aware operation of the D2D network, and the feasibility condition. The constraint in (3) is the classical necessity constraint for the queue stability describing the fact that the incoming rate to the network layer queues should be equal to or smaller than the outgoing service rate, which depends on the choice of the scheduling policy in our particular D2D communication scenario [29].[2]

In the next section, we will obtain the Pareto boundary of the network stability region, where no feasible and interference-aware scheduling policy can stabilize the D2D network when the arrival rates are beyond this boundary. This will provide a complete characterization of Λ. This characterization will be carried out under the full channel-state information (CSI) assumption. Although helpful in understanding the maximum rates that can be stably supported by a D2D network, such a characterization of the D2D network stability region does not provide us with any insights regarding how to design dynamic control mechanisms achieving the rates in Λ.

[2]Note that Λ is the minimal set that contains all achievable arrival rates, i.e., no vector $\boldsymbol{x}$ outside Λ can be stabilized by any feasible and interference-aware scheduling policy. Although not needed in our analysis, it is also important to note that it can be easily shown that the stability region Λ is a convex set by using the standard time-averaging arguments.

To resolve this drawback, we design a dynamic but centralized flow control and scheduling algorithm that achieves all the rates within the D2D network stability region in Section V. The scheduling part of the proposed algorithm provides design insights into how to construct a feasible and interference-aware scheduling mechanism for a D2D network. In addition to stabilizing an interference-aware D2D network, the proposed algorithm also maximizes the collective utility of the devices. The flow control part of the proposed algorithm provides design insights into how to construct flow control mechanism to maximize collective network performance. The distributed solutions achieving these desirable properties up to some provable performance bounds are given in Section VI.

IV. Stability Region for Interference-Aware D2D Network

In this section, we derive the boundary of the stability region of an interference-aware D2D network such that any arrival rate vector, $\boldsymbol{x}$ outside the closure of the boundary is unattainable. Then, we analyze the effect of interference-aware communication on the network stability region by comparing the boundaries obtained with and without interference constraints.

We begin our analysis by computing the boundary of network stability region. This is equivalent to maximizing the average outgoing (service) rate achieved by i for given average service rate values of other devices. Recall that the average arrival rate should be smaller or equal to the average service rate in a stable network. Hence, we say that any arrival rate of device i, x_i, that is larger than this maximized service rate, cannot be achieved. Before giving the mathematical description of the problem, we make following remark. Since we assume that the channels are ergodic and stationary, we utilize the statistical averages in constructing the optimization problem. Hence, we ignore the time index for the sake of notational simplicity in this section. But in the next section, when we perform dynamic control, we again introduce time index back. Further, for notational convenience, let $\Psi\in[0,1]^N$ be the set of all scheduling policies. Therefore, the aim is to maximize $\mathbb{E}\left[\mathscr{I}_i(\boldsymbol{h},\boldsymbol{g})R_i\right]$, associated with the point $\mathbb{E}\left[\mathscr{I}_j(\boldsymbol{h},\boldsymbol{g})R_j\right]=\alpha_j,\forall j\neq i$, by solving the following linear program:

$$\max_{\mathscr{I}\in\Psi}\mathbb{E}\left[\mathscr{I}_i(\boldsymbol{h},\boldsymbol{g})R_i\right] \tag{6}$$

$$\text{subject to}\ \mathbb{E}\left[\mathscr{I}_j(\boldsymbol{h},\boldsymbol{g})R_j\right]\geq\alpha_j,\ \forall j\neq i \tag{7}$$

$$\mathbb{E}\left[\sum_{l=1}^{N}P\mathscr{I}_l(\boldsymbol{h},\boldsymbol{g})g_l\right]\leq\gamma, \tag{8}$$

$$\sum_{l=1}^{N}Pg_l\mathscr{I}_l(\boldsymbol{h},\boldsymbol{g})\leq\nu\ \text{and}\ \sum_{l=1}^{N}\mathscr{I}_l(\boldsymbol{h},\boldsymbol{g})\leq 1, \tag{9}$$

where the expectations are over the joint distribution of the instantaneous channel gains of direct and interference channels. We solve the above optimization problem using the dual method that is particularly appealing to our problem structure, whose solution is given in the next theorem.

Theorem 1: The solution of the optimization problem given in (6)-(9) is given by

$$\mathscr{I}_j^*(\boldsymbol{h},\boldsymbol{g}) = \begin{cases} 1, & \text{if } W_j = \max_{1\le l\le N} W_l,\ \forall l \neq j \text{ and } W_j \ge 0 \\ & \text{and } Pg_j \le \nu \\ 0, & \text{otherwise} \end{cases} \tag{10}$$

where $W_j = \lambda_j^* R_j - \mu^* P g_j$ for all $j \neq i$ and $W_i = R_i - \mu^* P g_i$, and λ_j^* and μ^* are Langrange multipliers associated with the rate and interference constraints in (7) and (8) for which $\mathbb{E}\left[\mathscr{I}_j^*(\boldsymbol{h},\boldsymbol{g})R_j\right] = \alpha_j$, for all $j \neq i$ and the constraint in (8) is satisfied.

Proof: Please see Appendix A. ■

Theorem 1 gives us the optimal scheduling policy $\boldsymbol{\mathscr{I}}^*$ achieving $\mathbb{E}\left[\mathscr{I}_j^*(\boldsymbol{h},\boldsymbol{g})R_j\right] = \alpha_j$ for all $j \neq i$. Then, the boundary of the stability region can be attained by varying $\alpha_j, \forall j \neq i$, and obtaining the points where the average rates of device i are maximized. Another important point is that even though we state the optimization for the randomized scheduling policies, i.e., $\mathscr{I}_j(\boldsymbol{h},\boldsymbol{g}) \in [0,1]$, the optimal solution turns out to be a deterministic scheduling policy, i.e., $\mathscr{I}_j(\boldsymbol{h},\boldsymbol{g})$ is either zero or one. In addition, observe that if the condition $Pg_j > \nu$ and $W_j < 0$ for all i, then the channel remains idle, i.e., $\sum_{l=1}^N \mathscr{I}_l(\boldsymbol{h},\boldsymbol{g}) = 0$. The reason is that the channel conditions are not good enough to access the channel at the expense of the interference caused to the transmission of AP.

As indicated above, there may be time instants during which the channel remains idle in an interference-aware D2D network to safeguard the AP. This will result in a decrease in optimal rates due to under-utilization of the channel. Consequently, it leads to the contraction of the network stability region. To understand this phenomenon better, we also derive the optimum scheduling policy without interference constraints, and compare the achievable rate regions of both cases with and without interference constraints. Following similar arguments above, we have the following optimum scheduling problem

$$\max_{\boldsymbol{\mathscr{I}}\in\Psi} \mathbb{E}\left[\mathscr{I}_i(\boldsymbol{h},\boldsymbol{g})R_i\right] \tag{11}$$

$$\text{subject to } \mathbb{E}\left[\mathscr{I}_j(\boldsymbol{h},\boldsymbol{g})R_j\right] \ge \alpha_j,\ \forall j \neq i \text{ and } \sum_{l=1}^N \mathscr{I}_l \le 1 \tag{12}$$

without interference constraints, whose solution is given by the next lemma.

Lemma 1: The solution of the optimum scheduling problem in (11)-(12) is given as:

$$\mathscr{I}_j^*(\boldsymbol{h},\boldsymbol{g}) = \begin{cases} 1, & \text{if } \lambda_j^* R_j > \lambda_l^* R_l\ \forall l \neq j \\ 0, & \text{otherwise} \end{cases} \tag{13}$$

where λ_j^* is the Lagrange multiplier associated with the rate constraint in (12).

Proof: The proof follows the similar lines with the proof of Theorem 1, and hence is skipped to avoid repetitions. ■

Interpretation of Stability Network Region for Two Device Case: Now, we consider a communication scenario containing only two D2D pairs. In this case, the interference-aware optimum scheduling policy is given by

$$\mathscr{I}_1(\boldsymbol{h},\boldsymbol{g}) = \begin{cases} 1, & \text{if } R_1 - \mu^* P g_1 > \lambda^* R_2 - \mu^* P g_2 \text{ and } R_1 > \mu^* P g_1 \\ 0, & \text{otherwise} \end{cases}$$

and

$$\mathscr{I}_2(\boldsymbol{h},\boldsymbol{g}) = \begin{cases} 1, & \text{if } R_1 - \mu^* P g_1 < \lambda R_2 - \mu^* P g_2 \text{ and } \lambda^* R_2 > \mu^* P g_1 \\ 0, & \text{otherwise} \end{cases},$$

In Figs. 3a-3b, the stability region for a two-link D2D network, is illustrated for Rayleigh fading direct and interference channels. To plot the regions, we varied the rate achieved by the second D2D pair, and calculated λ^* and the boundary rate pair for each point. Recall that h_i and g_i are the direct and interference channel gains of ith D2D pair, respectively. In Fig. 3a, we take $\mathbb{E}[h_1] = \mathbb{E}[h_2] = 0.4$ and $\mathbb{E}[g_1] = \mathbb{E}[g_2] = 0.2$ and we obtain different boundary rate pair for varying interference parameter, γ. As seen in Fig. 3a, as we decrease γ value, i.e., the interference constraint is more stringent, both D2D pairs have smaller transmission opportunities to meet the interference constraint. Thus, the network stability region becomes smaller. In Fig. 3b, we fixed the value of γ at 0.1 and vary $\mathbb{E}[g_2]$. As seen in Fig. 3b, when $\mathbb{E}[g_2] = 0.1$, the network stability regions (with and without interference constraint) coincides for smaller values of R_1^{avg}, where the second D2D pair takes a higher portion of transmissions. In this case, the interference constraint is inactive since the second D2D pair with smaller interference channel gain transmits predominantly. On the other hand, as $\mathbb{E}[g_2]$ increases, i.e., $\mathbb{E}[g_2] = 0.2, 0.5, 1$, more interference is caused to the AP and the network stability region shrinks.

V. Control of Underlay D2D Communication Networks with Centralized Scheduling

In the previous section, we characterize the stability region by obtaining maximum rates that an interference-aware D2D network can support. In this section, we will present a dynamic control algorithm that will solve a network utility maximization (NUM) problem while stabilizing the network layer queues in a D2D network. To do so, we follow a cross-layer design approach. In the lower layer, the scheduling policy ensures network stability and satisfies the interference requirements. In the upper layer, on the other hand, flow control policy strives to move the network layer arrival rates to the optimal point within the stability region. Since the derived cross-layer algorithm will be a dynamic online algorithm, we will use the time index t in this section again to indicate its operation in time.

The dynamic cross-layer algorithm takes the queue lengths (both virtual and real queues) and instantaneous direct- and cross-channel gains as input, and determines the scheduled device i at each time slot as output. We start our analysis by first formulating the NUM problem and providing the queue dynamics to set the stage for the cross-layer design approach.

A. Problem Formulation

Our objective is to stabilize the network while maximizing the sum of device utilities. That is, we aim to find the solution of the following NUM problem:

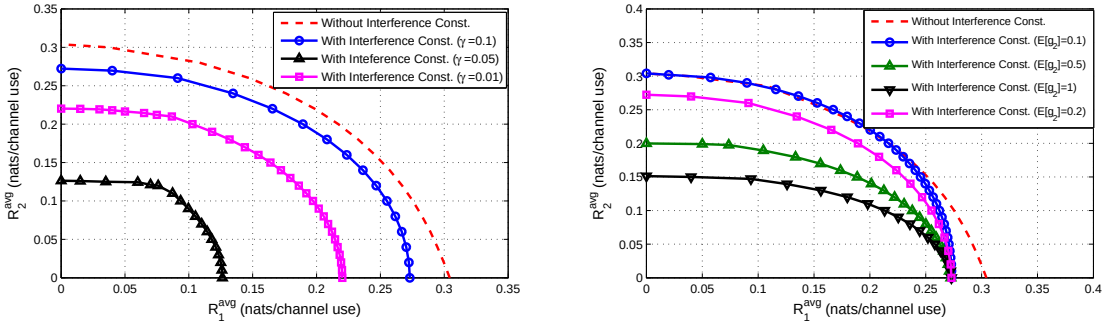

(a) Network stability region for varying interference parameter, γ (b) Network stability region for varying interference channel gain, $\mathbb{E}[g_2]$

Fig. 3. Network stability region for the communication scenario with two D2D pairs, where $R_i^{avg} = \mathbb{E}[\mathscr{I}_i^* R_i]$.

$$\max \sum_i U_i(x_i) \tag{14}$$

$$\text{subject to } x_i \in \Lambda \tag{15}$$

The objective function in (14) calculates the total expected utility of D2D pairs over random stationary channel conditions and scheduling decisions. The constraint (15) ensures that network layer arrival rates of D2D pairs are within the rate region supported by the network defined as Λ. The above problem could in principle be solved by means of standard convex optimization techniques if the stability region is known in advance. Although this approach may give us an idea about how to select transmission rates, it will not say anything about how we can reach the optimum operating by relating the solution to the design of wireless networks. Thus, in the following subsections, we develop a practical dynamic control algorithm to facilitate our understanding of the interplay between interference requirements of the D2D network and the critical functionalities of wireless networks, such as scheduling, and flow control.

B. Queue Dynamics

We assume that there is an infinite backlog of data at the transport layer of each node. Our proposed dynamic flow control algorithm determines the amount of traffic injected into the queues at the network layer. The dynamics of the network layer queue of ith D2D pair is given as follows:

$$Q_i(t+1) = [Q_i(t) - \mathscr{I}_i(t)R_i(t)]^+ + A_i(t). \tag{16}$$

To meet the average interference constraint given in (1), we also maintain a virtual queue as:

$$Z(t+1) = \left[Z(t) - \gamma + \sum_{i=1}^{N} \mathscr{I}_i(t) \cdot P g_i(t) \right]^+ \tag{17}$$

The state of the virtual queue at any given time instant is an indicator on the amount by which we exceed the allowable interference constraint. Thus, the larger the state of these queues, the more conservative our dynamic algorithm has to get towards meeting these constraints, i.e., the less transmissions will take place by D2D pairs. The strong stability of virtual queues guarantees that the interference constraints are satisfied in the long run (see Theorem 5.1 in [9]).

C. Dynamic Control

The proposed cross-layer dynamic control algorithm is based on the stochastic network optimization framework [9]. This framework allows the solution of a long-term stochastic optimization problem without requiring explicit characterization of the stability region. Furthermore, it enables the simultaneous treatment of stability and performance optimization by the introduction of virtual queues to transform performance constraints into queuing stability problems.

To this end, consider queue backlog vectors for D2D communication pairs as $\boldsymbol{Q}(t) = (Q_1(t), \ldots, Q_N(t))$ and $Z(t)$. Let $L(\boldsymbol{Q}(t), Z(t))$ be a quadratic Lyapunov function of real and virtual queue backlogs defined as:

$$L(\boldsymbol{Q}(t), Z(t)) = \frac{1}{2}\left((Z(t))^2 + \sum_{i=1}^{N} (Q_i(t))^2 \right). \tag{18}$$

Also, consider the one-step expected Lyapunov drift, $\Delta(t)$ for the Lyapunov function as:

$$\Delta(t) = \mathbb{E}\left[L(\boldsymbol{Q}(t+1), Z(t+1)) - L(\boldsymbol{Q}(t), Z(t)) | \boldsymbol{Q}(t), Z(t) \right].$$

The aim of stochastic optimization framework is to minimize the drift to ensure the network stability, which can be achieved by having negative Lyapunov drift whenever the sum of queue backlogs is sufficiently large. Intuitively, this property ensures network stability because whenever the queue backlog vector leaves the stability region, the negative drift eventually drives it back to this region. Furthermore, the following utility-mixed Lyapunov drift

$$\Delta^U(t) = \Delta(t) - V\mathbb{E}\left[\sum_{i=1}^{N} U_i(A_i(t)) | \boldsymbol{Q}(t), Z(t) \right], \tag{19}$$

enables us to maximize the network performance in conjunction with the network stability, where the conditional expectation is taken with respect to the random fading realizations.

Next, we present the control algorithm that minimizes (19) and provide its optimality in Theorem 2.

Control Algorithm: Making an analogy to back pressure algorithm, we propose the following cross-layer algorithm which executes the following steps in each time t:

(1) Upper Layer - Flow control: The flow controller at each device observes its current queue backlog, $Q_i(t)$. It then injects $A_i(t)$ bits, where $A_i(t)$ is the solution of the following optimization:

$$A_i(t) = \underset{0\le x\le A_{max}}{\operatorname{argmax}} \{VU_i(x) - Q_i(t)x\}, \tag{20}$$

where $V > 0$ is a design constant that will determine the final performance of the designed algorithm. The above identity involves maximizing a concave function, which can be easily solved by using convex optimization techniques [30].

(2) Lower Layer - Scheduling: A scheduler observes the backlogs in all devices, and all fading states. Then, it determines the scheduling decision for time slot t, $\mathscr{I}(t)$ as the solution of the following optimization:

$$\mathscr{I}(t) = \underset{\mathscr{I}\in\Psi}{\operatorname{argmax}} \left\{\sum_{i=1}^{N} \mathscr{I}_i W_i(t)\right\}$$
$$\text{subject to } \sum_{i=1}^{N} \mathscr{I}_i W_i(t) \le 1 \text{ and } \mathscr{I}_i P g_i(t) \le \nu,\ \forall i,$$

where $W_i(t)$ is the weight of pair i and is given as:

$$W_i(t) = Q_i(t)\mathscr{I}_i(t)R_i(t) - Z(t)Pg_i(t). \tag{21}$$

The above is a standard linear optimization problem, whose solution is obtained on the boundary. Specifically, among the pairs that satisfies the instantaneous interference constraint, and has the maximum weight, is allowed to transmit at a given time slot.

We note that the parameter V in the flow control algorithm that determines the extent to which the utility optimization is emphasized. Indeed, if V is large relative to the current backlog in the source queues, then the admitted rates $A_i(t)$ will be large, increasing the time average utility while consequently increasing congestion. This effect is mitigated as the backlog grows at the source queues and flow control decisions become more conservative. Note that the flow control algorithm is decentralized because the control values for each node require only knowledge of the queue backlogs in device i.

In the scheduling policy, the weight equation in (21) consists of reward $Q_i(t)R_i(t)$ and cost $PZ(t)g_i(t)$ terms. Specifically, the larger the data queue backlog size $Q_i(t)$ and/or higher the instantaneous channel rate $R_i(t)$, the more likely the transmission of D2D pair i occurs. On the other hand, larger the interference queue backlog $Z(t)$ (representing the interference level caused to AP) and/or higher the interference channel gain $g_i(t)$, the less likely the transmission of pair i takes place. In this setting, the flow control algorithm strives to maximize collective network utility, whereas the scheduling policy makes sure that the utility maximizing operating point is within the stability region. Indeed, by utilizing the proposed scheduling algorithm, we can achieve any point in the stability region.

Theorem 2: Suppose $\boldsymbol{x^*} = [x_1^*, \ldots, x_N^*]$ is the average arrival rates produced by the proposed dynamic control algorithm. Then, for any flow parameter $V > 0$, the dynamic control algorithm yields the following performance bound for the aggregate network utility:

$$\sum_{i=1}^{N} U_i(x_i^*) \ge U^* - \frac{B_1}{V}$$

while bounding the total long-term expected queue lengths as:

$$\limsup_{T\to\infty} \frac{1}{T}\sum_{\tau=0}^{T-1}\sum_{i=1}^{N} \mathbb{E}[Q_i(\tau)] \le \frac{B_1 + V\kappa}{\varepsilon_1},$$

where $B_1, \varepsilon_1, \kappa > 0$ are constants, and U^* is the optimal aggregate utility, i.e., the solution of the problem in (14)-(15). This theorem shows that the proposed dynamic control gets arbitrarily close to the optimal utility by choosing V sufficiently large at the expense of proportionally increased average queue sizes.

Proof: The proof is given in Appendix B. ■

We note that the proposed dynamic control algorithm is not distributed since its scheduling part depends on global queue length information. As compared to the distributed scheduling algorithms, the centralized scheduling schemes usually lead to a better performance at the cost of requiring a central authority to allocate the network resources. In a large-scale wireless network, such a central authority does not always exist. Furthermore, implementation of the centralized algorithms results in high overhead on the network due to collecting channel conditions and queue states of all users. In the remainder of the paper, we focus on designing distributed algorithms relaxing the assumptions necessary for the centralized algorithm. Note that the flow control part of the proposed solution is already distributed, i.e, each node decides its admitted flow by only local information. Thus, they remain the same below.

VI. Channel-Aware Distributed Algorithms

In this section, we relax the requirement of having a central authority for device scheduling in Section V by investigating contention based distributed scheduling algorithm with multiple round contention, called Channel-Aware Distributed Schedulers (CADS) with uniform mapping, that operates based on the local queue size and channel state information at each D2D pair. The distributed mode of operation necessitates the modification of the NUM problem as

$$\max \sum_i U_i(x_i) \tag{22}$$

$$\text{subject to } x_i \in \alpha\Lambda \tag{23}$$

where α is the contraction coefficient. The constraint in (23) suggests that the distributed scheduling algorithms can still stabilize the network, provided that the arrival rates are interior to $\alpha\Lambda$, which is a α scaled version of the stability region.

In the remainder of the section, we will introduce a distributed scheduling algorithm that is channel-aware in the sense that they can utilize the diversity gain in time-varying environments, and obtain its performance bounds by characterizing α. For analytical purposes, we assume that all channel gains, $h_i(t)$ and $g_i(t)$ are i.i.d. However, we perform simulations for i.i.d and non-i.i.d. cases and observe that the proposed algorithm often achieves scheduling performance far better than the obtained performance *lower* bounds. Furthermore, we

will only assume the average interference constraint, but it is straightforward to incorporate the instantaneous interference requirement in the solutions.

A. Contention Resolution Phase in CADS

In this part, we introduce the common operational principles shared by all CADS-type distributed schedulers that will be introduced in the subsequent sections. Operation of a CADS takes place in slotted time in two phases: (i) contention phase and (ii) data transmission phase. The contention phase is composed of M mini-slots, each of which is of enough duration to detect contention signals from other devices, i.e., a mini-slot must be at least 8μs in IEEE 802.11b. If τ is the ratio of the mini-slot duration to the duration of a regular time slot, then the parameter $M\tau$, which will appear in our derivations below, signifies the fraction of time spent to resolve collisions by means of implementing a contention resolution phase before the transmission of actual data.

The contention from devices for the time slot t is resolved as follows. The ith D2D pair selects a mini-slot $m \in \{1,\dots,M+1\}$ to send its contention signal. The selected mini-slot m depends on the pair i's weight $W_i(t)$ that incorporates queue backlog, direct channel and interference channel information into a single parameter. If pair i senses a contention signal from another pair before the mth mini-slot, it stops contending for the channel and defers its data transmission to the next time slot, i.e., $\mathscr{I}_i(t)=0$. Otherwise, it sends a contention signal in the beginning of the mth mini-slot. If no collision is sensed, the ith D2D pair obtains the access for the channel to transmit its data for the remaining part of the time slot, called the data transmission phase, commencing after the contention phase. If a collision is sensed, then the time slot remains idle and no data transmission takes place. These steps are visually illustrated in Fig. 4 and summarized in Algorithm 1 below.

Secondly, we assume that when a D2D pair detects a contention from other devices, it stops contenting the channel, i.e., the first pair which contends for the channel, obtains the right to access the channel and start transmitting in data transmission phase as illustrated in Fig. 4a. Furthermore, if more than one user contend in the same mini-slot, we say that collision takes place and the channel remains idle in data transmission phase as illustrated in Fig. 4b to prevent redundant interference to AP. The basic operational steps of CADSs is summarized in Algorithm 1.

Based on the contention resolution algorithm in CADS described above, the D2D pair with the smallest backoff time earns the access rights for the channel. Hence, it is of critical importance to design an efficient association policy mapping smaller backoff times to the larger weights $W_i(t)$ to ensure high utility and to exploit multiuser diversity. Our aim below is to investigate the structure of such efficient policies associating device weights with the mini-slot indices.

Definition 4: A mini-slot association policy $\boldsymbol{\Theta}(\boldsymbol{x}) = [\Theta_1(x_1),\dots,\Theta_N(x_N)]$ is a mapping $\boldsymbol{\Theta}:\mathbb{R}_+^N \mapsto \{1,\dots,M+1\}^N$ such that its ith component function $\Theta_i(x_i)$ determines the mini-slot index to which the ith pair is assigned given that $W_i(t)=x_i$.

Algorithm 1 Contention Resolution in CADS

1. At the beginning of each time slot t, the pair i picks a mini-slot $m \in \{1,\dots M\}$ based on its weight $W_i(t)$.
2. If a contention signal is heard before the mth mini-slots, then the pair i suspends its contention, it will set $\mathscr{I}_i(t)=0$.
3. If no contention signal is heard, the pair i transmits a contention signal at the beginning of the $m$the mini-slot.
- If a collision is detected, the pair i sets $\mathscr{I}_i(t)=0$.
- If no collision is detected, the pair i sets $\mathscr{I}_i(t)=1$, and starts its transmission at the beginning of data transmission phase.
4. The whole process restarts in the next time slot.

Further, $\boldsymbol{\Theta}$ is said to be a threshold policy if all of its component functions can be written as

$$\Theta_t^{(i)}(x)=\begin{cases} m, & \text{if } a_m^{(i)}(t)\le x < a_{m-1}^{(i)}(t), \quad \text{for } m\in\{1,\dots,M\} \\ M+1, & \text{if } W_i(t)<0, \end{cases}$$

where $\Theta_t^{(i)}(x)=M+1$ indicates that the pair i does not contend for the channel in time slot t.

Note that the input of mapping function is the weight of devices, $W_i(t)$. Hence, if $W_i(t)<0$, the transmission of the pair i causes more harms to the AP by injecting excessive interference compared to the benefit of the data transmission.

Below, we design a threshold-based mini-slot association policy in which the goal is to operate in close proximity of optimal point without imposing high complexity, and to provide fairness between D2D pairs. Furthermore, in numerical section, we compare the performance of the designed policy with different threshold-based mini-slot association policies that mainly differ on determining the threshold values $a_m^{(i)}(t)$.

B. CADS with Uniform Mapping

In CADS with uniform mapping, each pair is assigned to a mini-slot uniformly at random over all available mini-slots. This is achieved by utilizing the distribution of weights $W_i(t)$ of pairs as follows. [3] Let $F_{i,t}(x)$ is the conditional cumulative distribution function (CDF) of $W_i(t)$ at time slot t given that $W_i(t)$ is larger than zero, and let $f_{i,t}(x)$ be the corresponding probability density function (PDF). Given $Q_i(t)$ and $Z(t)$, each device can obtain $F_{i,t}(x)$ as follows:

$$F_{i,t}(x)=\mathbb{P}\left(W_i(t)\le x | W_i(t)>0, Q_i(t), Z(t)\right) \qquad (24)$$

Furthermore, let $(F_{i,t})^{-1}(\cdot)$ be the inverse function of $F_{i,t}(\cdot)$. The following lemma indicates how to select the threshold values $a_m^{(i)}(t)$ to achieve uniform distribution over all mini-slot indices.

Lemma 2: In CADS with uniform mapping, the mapping function, $\boldsymbol{\Theta}_t$, is as follows:

$$\Theta_t^{(i)}(x)=\begin{cases} m, & \text{if } (F_{i,t})^{-1}\left(\frac{M-m}{M}\right)\le x < (F_{i,t})^{-1}\left(\frac{M-m-1}{M}\right), \\ & \qquad\qquad \text{for } m\in\{1,\dots,M\} \\ M+1, & \text{if } W_i(t)<0, \end{cases}$$

[3] In our model, the fading process is stationary and independent from slot to slot. Hence, the D2D pairs know their instantaneous channel gains, and can learn channel distributions by observing the channel over a period of time [31].

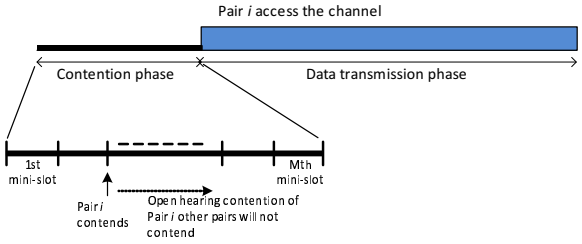
Pair i access the channel
Contention phase
Data transmission phase
1st mini-slot
Mth mini-slot
Pair i contends
Open hearing contention of Pair i other pairs will not contend

(a) Successful Contention

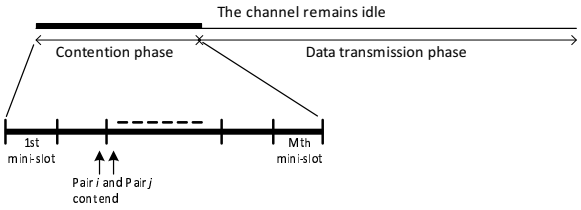

(b) Collision in Contention Phase

Fig. 4. Illustration of Algorithm 2

The mini-slot association policy above ensures that each pair picks a mini-slot uniformly at random, i.e., with a probability $\frac{1}{M}$ given that its weight is positive. The goal here is to minimize the probability collisions by spreading the contention probabilities uniformly over all mini-slots. Furthermore, this mini-slot association policy also enforces the scheduling of schedule a good D2D pair with respect to the current channel and queue states. However, it should be noted that such a uniform mapping policy, although promising, does not necessarily guarantee the scheduling of the best user, i.e., the user that has the maximum weight, as discussed subsequently.

C. Performance Analysis of CADS with Uniform Mapping

Here, we characterize the performance of CADS with uniform mapping by studying the performance loss due to fraction of time allocated to the contention resolution period, collisions in the contention period and imperfect scheduling.

1) *Performance Loss Due to Contention Period*: We assume that the length of mini-slots is not negligible. Hence, the devices that are scheduled to transmit, can only use $1-M\tau$ fraction of a whole time slot. That is the loss due to a contention resolution phase with multiple mini-slots, is $M\tau$.

2) *Performance Loss Due to Collisions in the Contention Phase*: The CADS with uniform mapping cannot prevent collision in the contention phase perfectly. Whenever such a collision occurs, all D2D pairs remain silent during the data transmission phase, and the channel becomes under-utilized. In the sequel, we characterize this loss.

3) *Performance Loss Due to Imperfect Scheduling*: The CADS with uniform mapping does not always schedule the D2D pair that has the maximum weight. The main underlying reason behind this phenomenon is that each device is assigned to a mini-slot uniformly at random with respect to their respective weights. Although this provides fairness among devices in giving the access rights to the channel (i.e., devices with lower and higher weights are treated equally), it can lead to assignment of channel access rights to the devices with smaller weights. Let us define the expected loss due to such an imperfect scheduling as β, where $0 \leq \beta \leq 1$.

We do not try to characterize β analytically for arbitrary number of devices and mini-slots due to intractability of calculations. Hence, β will appear as a parameter in Theorem 3 determining the performance of the CADS with uniform mapping. Our simulation results indicate that the loss due to imperfect scheduling is negligibly small for i.i.d. channels.

We need the following lemma to characterize the performance of the CADS with uniform mapping.

Lemma 3: The CADS with uniform mapping satisfies the following inequality:

$$\mathbb{E}\left[\sum_{i=1}^{N} \mathscr{I}_i(t) W_i(t)\right] \geq \mathbb{E}[W^*(t)]\,\alpha.$$

where $\alpha = (1-M\tau)(1-\beta)\left(\frac{N}{M}\sum_{k=1}^{M}\frac{N(M-k)^{N-1}}{(M-k+1)^N-(M-k)^N}\right)$

Proof: The proof is given in Appendix C. ∎

Lemma 3 indicates that the sum of average weights achieved by the uniform mini-slot association policy is larger than a fraction of the maximum weight. By using Lemma 3, we next characterize the performance of the CADS with uniform mapping.

Theorem 3: Suppose $\boldsymbol{x}^* = [x_1^*, \ldots, x_N^*]$ is the average arrival rates produced the CADS with uniform mapping. Then, for any flow parameter $V > 0$, the algorithm achieves the following performance bound:

$$\sum_{i=1}^{N} U_i(x_i^*) \geq \alpha U^* - \frac{B_2}{V}$$

while bounding the long-term expected queue lengths as:

$$\limsup_{T\to\infty} \frac{1}{T}\sum_{\tau=0}^{T-1}\sum_{i=1}^{N}\mathbb{E}[Q_i(\tau)] \leq \frac{B_2 + V\kappa}{\varepsilon_3},$$

where $B_2, \varepsilon_3, \kappa > 0$ are constants, and U^* is the optimal aggregate utility, i.e., the solution of the problem in (14)-(15).

Proof: The proof follows from Corollary 5.2 in [9] in the light of information given in Lemma 3, and given in Appendix D. ∎

VII. Numerical Results

A. Simulation Setup and Parameters

In our numerical experiments, we consider a two-tier network, in which D2D pairs are communication with each other while causing interference to CBS. Furthermore, we consider logarithmic utility function for all D2D pairs [4]. Specifically, pair i obtains utility of $\log(1+x_i)$ at the rate of x_i. The rates depicted in the graphs are the sum of arrival rates of all users and the unit of the plotted rates is natts/channel use. First, the main channel between D2D pairs and interference channel between transmitters of pairs are modeled as i.i.d. Rayleigh fading Gaussian channels. Thus, the main and interference

[4]We utilize logarithmic utility function to provide proportional fairness.

power gains are exponentially distributed with means 2 and 1, respectively. The noise normalized power is $P=1$. Furthermore, in experiments, we only consider average interference constraint. We compare the performance of our algorithm with different mini-slot association policies and that of widely used regulated queue approach.

1) CADS with Optimal Weight Mapping: In this subsection, we design a mapping function such that it maximizes the expected weight of D2D pairs by neglecting the effect of the imperfect scheduling. That is to say, the sequence of threshold value is determined as the solution of the following optimization problem:

$$\max_{a_m} \mathbb{E}[\mathscr{I}_i(t)W_i(t)] = \sum_{m=1}^{M} \mathbb{E}[\mathscr{I}_i(t)W_i(t)|\Theta(W_i(t))=m]$$

Since the above optimization problem is highly non-linear and dependent on distribution of fading process, we are not able to obtain closed-form solution. Hence, we numerically solve the problem in the numerical result section. Furthermore, obtaining the performance bound on this mapping function is non-trivial due to having no access to closed-form solution. However, we should note that since the algorithm maximizes the sum of weights, it results in better bounds obtained for the one with uniform mapping given in Lemma 3 and Theorem 3. Hence, it results in better performance compared to uniform mapping at the expense of high complexity.

2) CADS with Linear Mapping: In this section, we explicitly consider this practical challenge and propose an easily implementable and efficient algorithm for the users having limited power and memory. This time, we utilize a liner mapping discrete mapping function Θ, is defined as follows:.

$$\Theta(W_i(t)) = \begin{cases} m, & \text{if } \frac{(M-m-1)W_{max}}{M} \leq W_i(t) < \frac{(M-m)W_{max}}{M}, \\ & \text{for } m \in \{1,\ldots,M\} \\ M+1, & \text{if } W_i(t) < 0, \end{cases}$$

where W_{max} is ideally a value that the the number of realization of $W_i(t)$ which are larger than W_{max}, is small. However, since we assume that the users are not capable of calculating the mapping according the distribution function, they agree a value for W_{max}.

3) Interference Regulated Distributed Scheduler: In the sequel, we modify the regulated queue model to consider the interference constraint, and it is called Interference Regulated Distributed Scheduler (IRDS), which is based on the baseline algorithm in [32].

The operation of IRDS again has again two phases: (i) contention phase and (ii) data transmission phase. To facilitate the discussion, we introduce two new random variables related to contention and scheduling phases. The first one is the contention variable, $a_i(t)$, that is 1 with probability $\frac{1}{N}$, and 0 with probability $\frac{N-1}{N}$. The second one is the transmission variable, $p_i(t)$, that is 1 with probability $\frac{e^{W_i(t)}}{e^{W_i(t)}+1}$, and 0 with probability $\frac{1}{e^{W_i(t)}+1}$, where $W_i(t)$ is the weight of D2D pair i defined in (21). We note that the transmission variable takes also into account interference level that is caused to AP. This is the reason why, the algorithm is regulated with respect to the interference level.

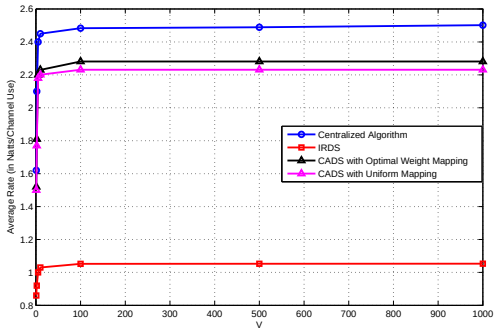

Fig. 5. Performance Analysis of Algorithms with respect to V

The scheduling decision of D2D pair i depends on the following three conditions:

Condition (1): The contention of pair i is successful, i.e., $a_i(t)\prod_{j\neq i}(1-a_j(t))=1$.

Condition (2): None of the neighboring pairs were scheduled in the previous time slot, i.e., $\sum_{j\neq i}\mathscr{I}_j(t-1)=0$

Condition (3): The transmission variable $p_i(t)=1$.

Based on these three conditions, the scheduling phase consists of three different cases, as given by Algorithm 2.

Algorithm 2 Scheduling Phase of IRDS

Each D2D pair schedules $\mathscr{I}_i(t)$ according to
Case 1: $\mathscr{I}_i(t)=1$ if Conditions (1)(2)(3) holds.
Case 2: If Condition (1) does not hold and Condition (3) holds, then $\mathscr{I}_i(t)=\mathscr{I}_i(t-1)$.
Case 3: Otherwise, $\mathscr{I}_i(t)=0$.

Notice that IRDS only consider single round contention unlike the proposed CADSs, which limits the performance of the algorithm as shown in simulation results.

B. Simulation Results

In Fig. 5, we investigate the effect of system parameter V in our dynamic control algorithms. We take interference constraint, $\gamma=1$ and the ratio of length of a mini-slot to the length of a slot is taken as 0.0001, i.e., $\tau=0.0001$. Furthermore, the number of mini-slots, M, is 200. As expected, the average rate of all algorithms increase with increasing V and Fig. 5 shows that the long-term utilities for $V\geq$ converges to their optimal values fairly closely verifying the results in Theorem 1. Furthermore, the distributed algorithm with the best performance is CADS with optimal weight mapping achieving over 90% of the average rate of centralized algorithm. CADS with uniform mapping exhibits a performance fairly close to the one with optimal weight mapping. However, IRDS is the distributed scheduler with worst performance achieving only approximately 40% of the average rate of centralized algorithm.

For the rest of the experiments, we take $V=200$. In Fig. 6a and 6b, we anaylze the effect of interference constraint, γ, number of D2D pairs, N, on the system performance, respectively. As illustrated in Fig. 6a, the average rate for all

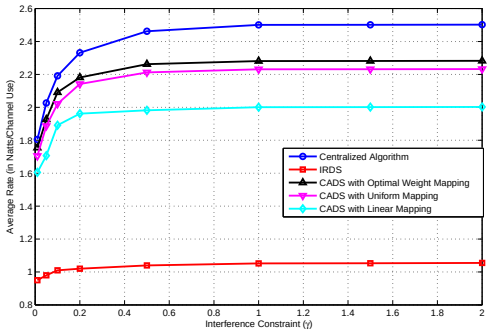

(a) Performance with respect to γ, γ

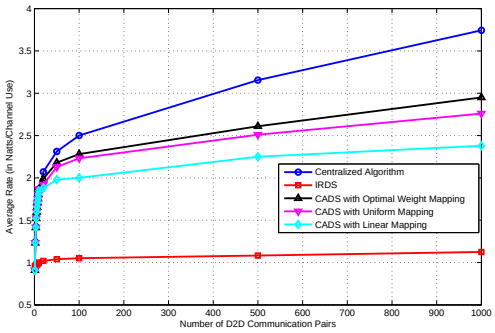

(b) Performance with respect to N, $\mathbb{E}[g_2]$

Fig. 6. Performance Analysis of Algorithms with respect to γ and N

algorithms increases with increasing γ. This is because for low γ values, in order to satisfy a tight interference constraint, a larger fraction of time-slots remains idle, i.e., smaller number of transmission opportunities are given to D2D pairs. Starting around $\gamma = 1$, the interference constraint becomes inactive, since the constraint is realized with strict inequality. From Fig 6b, we first notice that the performance of IRDS does not change with the increasing number of pairs and only achieves %90 of the rate achieved by the centralized algorithm when the number of pairs is one. Thus, we can conclude that IRDS cannot take advantage of diversity gain of fading channels. On the other hand, CADS with optimal weight, uniform and linear mapping achieves a performance that is closer to the centralized algorithm. As expected, CADS with optimal weight mapping performs the best whereas the one with linear mapping has the worst performance. In linear mapping, we sacrifice some performance in favor of reducing the complexity of mapping. Furthermore, as the number of pairs increases, the collisions during contention phase increases. This results in an increase in the difference between the performance of centralized and CADSs.

Next, we analyse the effect of the number of mini-slots on the performance of CADSs. We take the number of SUs as 100. In Fig. 7a, we take $\tau = 0.0001$ and in Fig. 7b, we take $\tau = 0.002$. As illustrated in Fig. 7a, the average data rate increases initially with increasing M. This is due to fact with increasing M, the network experiences less collision. However, when M is high, the emphasis on reducing collisions becomes less significant, and the loss due to length of contention phase, i.e., $M\tau$ increases. As a result, the performance of CADSs gets worse. The optimal M is achieved when M is around 600. In Fig. 7b, we notice that the optimal M is around 400 and the decrease of the average rate due to having long contention phase is sharper compared to the case when $\tau = 0.0001$.

Lastly, we investigate the performance of algorithms with respect to γ and number of D2D pairs, N, when the channels are non-iid. Precisely, the main and interference channel gains of D2D pairs are chosen at random, uniformly distributed in the intervals [1.2, 2.8], and [0.2,1.8], respectively. In addition, we take 10 runs and the rates depicted in Fig. 8a and 8b are the average of these 10 runs. From Fig. 8a and 8b, we notice that CADS with optimal weight and uniform mappings perform slightly worse compared to the case when the channel gains are iid. The reason is that when the channel gains are non-iid, the algorithms do not schedule the pair with the highest weight in high number of instances frequency due to having different mapping interval for each pair.

VIII. Conclusion

In this paper, we considered the problem of resource allocation in wireless two-tier network where D2D communication pairs have information to be shared. However, the interference to the CBS should be kept arbitrarily low caused by the transmission between D2D pairs. First, we studied the stability region of such interference-aware network, and compare the region to the case when there is no interference constraint. Then, we described a cross-layer dynamic algorithm, and we proved that our algorithm achieves utility arbitrarily close to achievable optimal utility.

Finally, we investigate distributed algorithms, where each pair decides to transmit or not according to local information. We design a channel-aware distributed scheduling algorithm, which is a threshold based mini-slot association policy. We derive the performance bound achieved by this algorithm, and compare the performance of the proposed algorithm with widely used regulated queue approach and different mini-slot association policies. Via simulations, we show that the proposed algorithm achieves high performance, and the reduction in average rate in the proposed algorithms due to implementing distributed approach is relatively small.

References

[1] L. Lei, Z. Zhong, C. Lin, and X. Shen, "Operator controlled device-to-device communications in lte-advanced networks," *IEEE Wireless Commun. Mag.*, vol. 19, no. 3, pp. 96–104, Jun. 2012.

[2] G. Fodor, E. Dahlman, G. Mildh, S. Parkvall, N. Reider, G. Miklos, and Z. Turanyi, "Design aspects of network assisted device-to-device communications," *IEEE Commun. Mag.*, vol. 50, no. 3, pp. 170–177, Mar. 2012.

[3] L. Tassiulas and A. Ephremides, "Jointly optimal routing and scheduling in packet ratio networks," *IEEE Transactions on Information Theory*, vol. 38, no. 1, pp. 165 –168, Jan. 1992.

[4] X. Liu, E. K. P. Chong, and N. B. Shroff, "A framework for opportunistic scheduling in wireless networks," *Computer Networks*, vol. 41, no. 4, pp. 451–474, 2003.

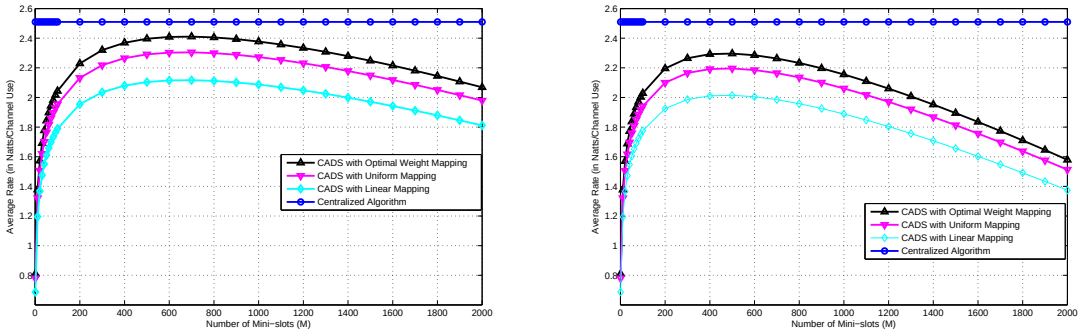
Average Rate (in Nats/Channel Use)
Number of Mini−slots (M)
CADS with Optimal Weight Mapping
CADS with Uniform Mapping
CADS with Linear Mapping
Centralized Algorithm

(a) $\tau = 0.0001$, γ (b) $\tau = 0.0002$, $\mathbb{E}[g_2]$

Fig. 7. Performance Analysis of CSMA-based distributed algorithms with respect to the ratio of length of mini-slots to the one of slot.

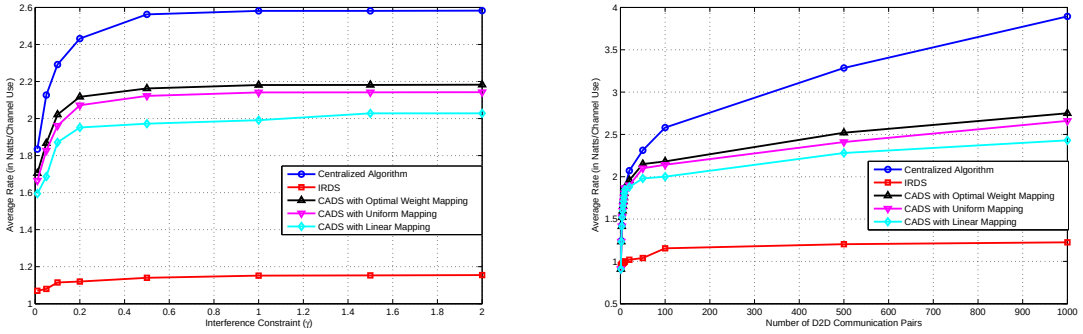

(a) Performance with respect to γ, γ (b) Performance with respect to γ, $\mathbb{E}[g_2]$

Fig. 8. Performance Analysis of Algorithms with respect to γ and N with non-iid channels

[5] R. Urgaonkar and M. J. Neely, "Opportunistic scheduling with reliability guarantees in cognitive radio networks," *IEEE Trans. Mob. Comput.*, vol. 8, no. 6, pp. 766–777, 2009.

[6] J. J. Jaramillo and R. Srikant, "Optimal scheduling for fair resource allocation in ad hoc networks with elastic and inelastic traffic," in *INFOCOM*, 2010, pp. 2231–2239.

[7] F. P. Kelly, A. K. Maulloo, and D. K. H. Tan, "Rate Control for Communication Networks: Shadow Prices, Proportional Fairness and Stability," *The Journal of the Operational Research Society*, vol. 49, no. 3, pp. 237–252, 1998. [Online]. Available: http://dx.doi.org/10.2307/3010473

[8] X. Wang and K. Kar, "Cross-layer rate control for end-to-end proportional fairness in wireless networks with random access," in *MobiHoc*, 2005, pp. 157–168.

[9] L. Georgiadis, M. J. Neely, and L. Tassiulas, "Resource allocation and cross-layer control in wireless networks," *Foundations and Trends in Networking*, vol. 1, no. 1, 2006.

[10] C. H. Yu, O. Tirkkonen, K. Doppler, and C. B. Ribeiro, "On the performance of device-to-device underlay communication with simple power control," in *in Proc. IEEE Vehicular Technology Conf. (VTC)*, Apr. 2009, pp. 1–5.

[11] C. H. Yu, K. Doppler, C. Riberio, and O. Tirkkonen, "Resource Sharing Optimization for Device-to-Device Communication Underlaying Cellular Communication," *IEEE Transactions on Wireless Communications*, vol. 10, no. 8, pp. 2752–2763, 2011.

[12] P. Janis, C. Yu, K. Doppler, C. Ribeiro, C. Wijting, K. Hugl, O. Tirkkonen, and V. Koivunen, "Device-to-device communication underlaying cellular communications system," *IEEE Trans. Inf. Theory*, vol. 2, no. 3, pp. 169–178, Mar. 2009.

[13] H. Min, J. Lee, S. Park, and D. Hong, "Capacity enhancement using an interference limited area for device-to-device uplink underlaying cellular networks," *IEEE Trans. Wireless Commun.*, vol. 10, no. 12, pp. 3995–4000, Dec. 2011.

[14] X. Xiao, X. Tao, and J. Lu, "A qos-aware power optimization scheme in ofdma systems with integrated device-to-device (d2d) communications," in *in Proceedings of IEEE VTC-Fall*, 2011, pp. 1–5.

[15] M. Jung, K. Hwang, and S. Choi, "Joint mode selection and power allocation scheme for power-efficient device-to-device (d2d) communication," in *in Proceedings of IEEE VTC-Spring*, 2012, pp. 1–5.

[16] S. Hakola, T. Chen, J. Lehtomaki, and T. Koskela, "Device-to-device (d2d) communication in cellular network-performance analysis of optimum and practical communication mode selection," in *in Proceedings of IEEE WCNC*, 2010, pp. 1–6.

[17] M. Belleschi, G. Fodor, and A. Abrardo, "Performance analysis of a distributed resource allocation scheme for d2d communications," in *in Proceedings of IEEE GLOBECOM Workshops*, 2011, pp. 358–362.

[18] D. F. et al., "Device-to-Device Communications Underlaying Cellular Networks," *IEEE Transactions on Communications*, vol. 61, no. 8, pp. 3541–3551, 2013.

[19] R. Zhang, X. Cheng, L. Yang, and B. Jiao, "Interference-aware graph based resource sharing for device-to-device communication underlaying cellular communication," in *in Proc. IEEE WNC*, 2013, pp. 140–145.

[20] L. Su, Y. Ji, P. Wang, and F. Liu, "Resource allocation using particle swarm optimization for d2d communication underlay of cellular networks," in *in Proceedings of IEEE WCNC*, 2013, pp. 129–133.

[21] B. G. K. M. H. Han and J. W. Lee, "Subchannel and transmission mode scheduling for d2d communication in ofdma networks," in *in Proceedings of IEEE VTC-Fall*, 2012, pp. 1–5.

[22] L. B. Le, "Fair resource allocation for device-to-device communications in wireless cellular networks," in *in Proceedings of IEEE GLOBECOM*, 2012, pp. 5451–5456.

[23] Q. W. et al., "Quality-optimized joint source selection and power control for wireless multimedia D2D communication using stackelberg game," *IEEE Transactions on Vehicular Technology*, vol. PP, no. 99, pp. 1–1, Sep. 2014.

[24] C. X. et al., "Efficiency resource allocation for device-to-device underlay communication systems: A reverse iterative combinatorial auction based

approach," *IEEE Journal on Selected Areas in Communications*, vol. 31, no. 9, pp. 348–358, Sept. 2013.
[25] Y. Li, D. Jin, J. Yuan, and Z. Han, "Coalitional games for resource allocation in the device-to-device uplink underlaying cellular networks," *IEEE Transactions on Wireless Communications*, vol. 13, no. 7, pp. 3965–3977, July 2014.
[26] H. Chen, D. Wu, and Y. Cai, "Coalition formation game for green resource management in D2D communications," *IEEE Communications Letterss*, vol. 18, no. 8, pp. 1395–1398, Aug. 2014.
[27] D. N. C. Tse and S. V. Hanly, "Multiaccess fading channelspart I: Polymatroid structure, optimal resource allocation and throughput capacities," *IEEE Trans. Inf. Theory*, vol. 44, no. 7, pp. 2796–2815, 1998.
[28] A. Goldsmith, S. A. Jafar, I. Maric, and S. Srinivasa, "Breaking spectrum gridlock with cognitive radios: An information theoretic perspective," *Proc. IEEE*, vol. 97, no. 5, pp. 894–914, 2009.
[29] M. J. Neely, "Optimal energy and delay tradeoffs for multi-user wireless downlinks," *Tech. Rep. CSI-05-06-01*, vol. University of Southern California, 2005.
[30] S. Boyd and L. Vandenberghe, *Convex Optimization*. New York, NY: Cambridge University Press, 2004.
[31] A. can der Vaart, *Asymptotic Statistics*. Cambridge , UK: Cambridge University Press, 1998.
[32] D. Xue and E. Ekici, "Efficient Distributed Scheduling in Cognitive Radio Networks in the Many-Channel Regime," *Wi-opt*, May 2013.
[33] Z. Latreuch and B. Beladi, "New inequalities for convexsequences with applications," *Int. J. Open Problems Comput. Math.*, vol. 5, no. 3, pp. 15–27, Sept. 2012.

APPENDIX A
PROOF OF THEOREM 1

The problem given in (6)-(9) leads to the following Lagrangian relaxation:

$$\min_{\lambda_j\geq 0,\mu\geq 0}\max_{\boldsymbol{\mathscr{I}}\in\Psi}\mathbb{E}\left[\mathscr{I}_i(\boldsymbol{h},\boldsymbol{g})R_i\right]+\sum_{j\neq i}\lambda_j\left(\mathbb{E}\left[\mathscr{I}_j(\boldsymbol{h},\boldsymbol{g})R_j\right]-\alpha_j\right)+\mu\left(\gamma-\sum_{l=1}^{N}\mathbb{E}\left[P\mathscr{I}_l(\boldsymbol{h},\boldsymbol{g})g_l\right]\right) \quad (25)$$

$$\text{subject to } \sum_{l=1}^{N}Pg_l\mathscr{I}_l(\boldsymbol{h},\boldsymbol{g})\leq \nu \text{ and } \sum_{l=1}^{N}\mathscr{I}_l\leq 1, \quad (26)$$

where we ignore α_j and γ in the expectation as they are merely constants and do not affect the solution.

Note that, since the channel rates are independently distributed, optimizing in each fading realization results in optimal solution of statistical averages in (25)-(26) in dual problem. That is to say, the solution, $I_j^*=I_j^*(\boldsymbol{h},\boldsymbol{g})$ will be a stationary policy, i.e., optimizing in each fading realization results in optimal solution of the problem. For any given values of the Lagrange multipliers, λ_j and μ, and transmission rate vector $(R_1,\ldots,R_N)$, the optimal policy will choose the scheduling decision in each time slot as the solution of the following Lagrangian problem:

$$\max_{\boldsymbol{\mathscr{I}}\in\Psi}\mathscr{I}_i(\boldsymbol{h},\boldsymbol{g})\left(R_i-\mu Pg_i\right)+\sum_{j\neq i}\mathscr{I}_j(\boldsymbol{h},\boldsymbol{g})\left(\lambda_jR_j-\mu Pg_j\right) \quad (27)$$

$$\text{subject to } \sum_{l=1}^{N}Pg_l\mathscr{I}_l((\boldsymbol{h},\boldsymbol{g})\leq \nu \text{ and } \sum_{l=1}^{N}\mathscr{I}_l\leq 1. \quad (28)$$

Since the above optimization problem has a linear objection function and constraints, we conclude that the optimization problem lies on the boundary. Specifically, for any given values of the Lagrange multipliers λ_j forall $j\neq i$ and μ, the optimal policy will be deterministic policy, i.e, $\mathscr{I}_j(\boldsymbol{h},\boldsymbol{g})\in\{0,1\}$. Furthermore, $\mathscr{I}_j(\boldsymbol{h},\boldsymbol{g})=0$ for all j, i. e., the channel remains idle, if $R_i-\mu Pg_i<0$ or $Pg_i>\nu$, and $\lambda_jR_j-\mu Pg_j<0$ or $Pg_j>\nu$ for all $j\neq i$. Also, for the duality gap to be zeo, the following KKT conditions should be satisfied for the optimal Lagrange multipliers [30]:

$$\mathbb{E}\left[R_i\right]+\sum_{j\neq i}\lambda_j^*\mathbb{E}\left[R_j\right]-\sum_{l=1}^{N}\mu^*P\mathbb{E}\left[g_l\right]=0, \quad (29)$$

$$\lambda_j^*\left(\mathbb{E}\left[\mathscr{I}_j^*R_j\right]-\alpha_j\right)=0,\forall j\neq i, \quad (30)$$

$$\mu^*\left(\gamma-\sum_{l=1}^{N}\mathbb{E}\left[P_l^*g_l\right]\right)=0,\mu^*\geq 0 \text{ and } \lambda_j^*\geq 0\forall j\neq i \quad (31)$$

The conditions in (30) and (31) express the fact that if a constraint is not active then its corresponding Lagrange multiplier is 0. Since the objective function, i.e., the rate achieved by D2D pair i is inversely proportional to the rates achieved by the other pairs. We conclude that $\lambda_j^*>0$ for all $j\neq i$ for which the corresponding constraint is realized with equality.

APPENDIX B
PROOF OF THEOREM 2

To derive the performance bound on the control algorithm, we start with providing an upper bound on $\Delta(t)$ in the following lemma.

Lemma 4:

$$\Delta(t)\leq B-\sum_{i=1}^{N}\mathbb{E}\left[Q_i(t)\left(\mathscr{I}_i(t)R_i(t)-A_i(t)\right)\mid Q_i(t)\right]-\mathbb{E}\left[Z(t)\left(\gamma-\sum_{i=1}^{N}Pg_i(t)\right)\mid Z(t)\right] \quad (32)$$

where $B>0$ is a constant.

Proof:

By using the bounds assumed for the channel rates and the arrival rates, the following inequalities can be obtained for each real queue:

$$\begin{aligned}&\mathbb{E}\left[(Q_i(t+1))^2-(Q_i(t))^2\mid Q_i(t)\right]\\&=\mathbb{E}\left[\left([Q_i(t)-\mathscr{I}_i(t)R_i(t)]^+ +A_i(t)\right)^2-(Q_i(t))^2\mid Q_i(t)\right]\\&\leq\mathbb{E}\left[Q_i(t)^2+A_i(t)^2+(\mathscr{I}_i(t)R_i(t))^2\right.\\&\left.-2Q_i(t)\left[\mathscr{I}_i(t)R_i(t)-A_i(t)\right]-Q_i(t)^2\mid Q_i(t)\right]\\&\leq C_1-2\mathbb{E}\left[\left(\mathscr{I}_i(t)R_i(t)-A_i(t)\right)\mid Q_i(t)\right],\end{aligned} \quad (33)$$

where $C_1=R_{max}^2+A_{max}^2$. The same line of derivation can be performed for the virtual queue to obtain

$$\mathbb{E}\left[Z(t+1)^2-Z(t)\right]\leq C_2-\mathbb{E}\left[Z(t)\left(\gamma-\sum_{i=1}^{N}Pg_i(t)\right)\mid Z(t)\right], \quad (34)$$

where $C_2=\gamma^2+n^2g_{max}^2$, and g_{max} is the bound on the first moment of the interference channel gain, $g_i(t)$, i.e., $\mathbb{E}\left[g_i(t)\right]\leq g_{max}$, for all $i=1,\ldots,N$.

Hence, by summing (33) over all $i=1,\ldots,N$ and (34), and multiplying with $\frac{1}{2}$, we obtain the upper bound on $\Delta(t)$ as given in the Lemma, where $B_1=\frac{n\left(R_{max}^2+A_{max}^2\right)+\gamma^2+n^2g_{max}^2}{2}$. ■

By using (32) in the lemma, we obtain an upper bound for (19), as follows:

$$\begin{aligned}\Delta^U(t) \le B_1 - V\mathbb{E}\left[\sum_{i=1}^{N} U_i(A_i(t))\right] - \sum_{i=1}^{N}\mathbb{E}\left[Q_i(t)\left(\mathscr{I}_i(t)R_i(t)-A_i(t)\right)\mid Q_i(t)\right]\\ -\mathbb{E}\left[\gamma - Z(t)\left(\sum_{i=1}^{N} Pg_i(t)\right)\mid Z(t)\right]\\ = B_1 - \sum_{i=1}^{N}\mathbb{E}\left[\left(U_i(A_i(t)-Q_i(t)A_i(t)\right)\mid Q_i(t)\right]\\ -\sum_{i=1}^{N}\mathbb{E}\left[\mathscr{I}_i(t)\left(Q_i(t)R_i(t)-Z(t)Pg_i(t)\right)\mid \boldsymbol{Q}(t),Z(t)\right]-\gamma \qquad (35)\end{aligned}$$

It is easy to observe that our proposed dynamic network control algorithm minimizes the right hand side of (35).

If there exists a feasible region, it has been shown in [9] that there must exist a stationary scheduling and rate control policy that chooses the users and the arrival rates independent of queue backlogs and only with respect to the channel statistics. In particular, the optimal stationary policy can be found as the solution of a deterministic policy if the channel statistics are known a priori.

Let U^* be the optimal value of the objective function of the problem ((14)-(15)) obtained by the aforementioned stationary policy. Also let ${x_i}^*$ be optimal traffic arrival rates found as the solution of the same problem. In particular, the optimal input rate ${x_i}^*$ could in principle be achieved by the simple backlog-independent admission control algorithm of including all new arrivals $A_i(t)$ for a given pair i in time t independently with probability $\zeta_i = {x_i}^*/x_i$. Then, the right-hand side (RHS) of (35) can be rewritten as:

$$\begin{aligned}B_1 - VU^* - \mathbb{E}[Q_i(t)]\,\mathbb{E}[\mathscr{I}_i(t)R_i(t)-A_i(t)]\\ -\mathbb{E}[Z(t)]\,\mathbb{E}[\gamma-\mathscr{I}_i(t)Pg_i(t)] \qquad (36)\end{aligned}$$

Also, since ${x_i}^*$ is in the achievable rate region, i.e., arrival rates are strictly interior of the rate region, there must exist a stationary scheduling and rate allocation policy that is independent of queue backlogs and satisfies the following:

$$\mathbb{E}[\mathscr{I}_i(t)R_i(t)] \ge {x_i}^* + \varepsilon_1 \text{ and } \sum_{i=1}^{N}\mathbb{E}[\mathscr{I}_i(t)Pg_i(t)] \le \gamma + \varepsilon_2 \qquad (37)$$

Note that as we consider stationary and ergodic policies, long-term averages (37) correspond to expectations of the same variables as in (35). Clearly, any stationary policy should satisfy (35). Recall that our proposed policy minimizes RHS of (35), and hence, any other stationary policy (including the optimal policy) has a higher RHS value than the one attained by our policy. In particular, the stationary policy that satisfies (37), and implements aforementioned probabilistic admission control can be used to obtain an upper bound for the RHS of our proposed policy. Inserting (37) into (36), we obtain the following upper bound for our policy:

$$RHS \le B_1 - \sum_{i=1}^{N}\varepsilon_1\mathbb{E}[Q_i(t)] - \varepsilon_2\mathbb{E}[Z(t)] - VU^*.$$

This is exactly in the form of Lyapunov Optimization Theorem given in [9], and hence, we can obtain bounds on the performance of the proposed policy and the sizes of queue backlogs as given in Theorem 2.

Appendix C
Proof of Lemma 3

Our aim here is to obtain a bound on the average weight achieved by CADS comparing with the weight achieved by the centralized algorithm given in Section V, i.e., the max weight algorithm. Also, we define the maximum weight, $W^*(t) = \text{argmax}_i W_i(t)\mathscr{I}_i(t)$. To characterize the bound, we first introduce the following probabilities:

$$\mathbb{P}(\Theta(W^*(t))=k) = \left(\prod_{n\le k}\left[1-\frac{1}{M-n+1}\right]^N\right)\left(1-\left[1-\frac{1}{M-k+1}\right]^N\right).$$

$$\begin{aligned}\mathbb{P}\left(\sum_{i=1}^{N}\mathscr{I}_i(t)=1,\Theta(W^*(t))=k\right) = \left(\prod_{n\le k}\left[1-\frac{1}{M-n+1}\right]^N\right)\\ \left(\binom{N}{1}\frac{1}{M-k+1}\left[1-\frac{1}{M-k+1}\right]^{N-1}\right).\end{aligned}$$

Note that $\sum_{i=1}^{N}\mathscr{I}_i(t)=1$ states that the contention phase takes place without a collision. Then, by using the above probabilities, we obtain the probability that the contention phase in CADS is successful given that the pair with the maximum weight contends in kth minislot as:

$$\begin{aligned}\mathbb{P}\left(\sum_{i=1}^{N}\mathscr{I}_i(t)=1\Big|\Theta(W^*(t))=k\right) = \frac{\mathbb{P}\left(\sum_{i=1}^{N}\mathscr{I}_i(t)=1,\Theta(W^*(t))=k\right)}{\mathbb{P}(\Theta(W^*(t))=k)}\\ = \frac{N(M-k)^{N-1}}{(M-k+1)^N-(M-k)^N}. \qquad (38)\end{aligned}$$

The collisions in first mini-losts result in higher performance loss compared to collisions in later mini-slots. Hence, the probability in (38) lets us to analyze the performance loss due to collisions in each mini-slot seperately.

Lemma 5: Let $P_k = \mathbb{P}\left(\sum_{i=1}^{N}\mathscr{I}_i(t)=1\Big|\Theta(W^*(t))=k\right)$. Then, the probability vector, $\boldsymbol{P} = (P_1,P_2,\ldots,P_M)$, is a monotonically descreasing convex sequence.

Proof: We omit the proof, since it is straightforward. It is enough to show that the first and second derivative of P_k with respect to k are negative. ■

Then, we bound the expected weight as:

$$\begin{aligned}\mathbb{E}\left[\sum_{i=1}^{N}\mathscr{I}_i(t)W_i(t)\right] = \mathbb{E}\left[(1-M\tau)(1-\beta)W^*(t)\sum_{i=1}^{N}\mathscr{I}_i(t)\right] \qquad (39)\\ = (1-M\tau)(1-\beta)\sum_{k=1}^{M}\mathbb{E}\left[W^*(t)\Big|\sum_{i=1}^{N}\mathscr{I}_i(t)=1,\Theta(W^*(t))=k\right]\\ \mathbb{P}\left(\Theta(W^*(t))=k,\sum_{i=1}^{N}\mathscr{I}_i(t)=1\right)\\ = (1-M\tau)(1-\beta)\sum_{k=1}^{M}\mathbb{E}\left[W^*(t)\Big|\sum_{i=1}^{N}\mathscr{I}_i(t)=1,\Theta(W^*(t))=k\right]\end{aligned}$$

$$\mathbb{P}\left(\Theta(W^*(t))=k\right)\mathbb{P}\left(\sum_{i=1}^{N}\mathscr{I}_i(t)=1\middle|\Theta(W^*(t))=k\right)$$
$$\leq\left(\sum_{k=1}^{M}\mathbb{E}\left[W^*(t)\middle|\sum_{i=1}^{N}\mathscr{I}_i(t)=1,\Theta(W^*(t))=k\right]\mathbb{P}\left(\Theta(W^*(t))=k\right)\right)$$
$$\left(\sum_{k=1}^{M}\frac{1}{M}\mathbb{P}\left(\sum_{i=1}^{N}\mathscr{I}_i(t)=1|\Theta(W^*(t))=k\right)\right)(1-M\tau)(1-\beta) \quad (40)$$
$$=\mathbb{E}\left[W^*(t)\right]\alpha, \quad (41)$$

where $\alpha=(1-M\tau)(1-\beta)\left(\frac{N}{M}\sum_{k=1}^{M}\frac{N(M-k)^{N-1}}{(M-k+1)^N-(M-k)^N}\right)$. (39) is by taking into account the loss due to imperfect scheduling and mini-slot implementation. (40) follows from Lemma 5 and the application of corallary 1.1. in [33]. Lastly, (41) follows from the following equality:

$$\mathbb{E}\left[W^*(t)\right]=\sum_{k=1}^{M}\mathbb{E}\left[W^*(t)\middle|\sum_{i=1}^{N}\mathscr{I}_i(t)=1,\Theta(W^*(t))=k\right]\mathbb{P}\left(\Theta(W^*(t))=k\right).$$

Appendix D
Proof of Theorem 3

The proof follows the similar lines of the proof of Theorem 2. Thus, we skip the first lines of the proof and write the one-step expected Lyapunov drift as:

$$\Delta(t)\leq B_2-\sum_{i=1}^{N}\mathbb{E}\left[Q_i(t)\left(A_i(t)-\mathscr{I}_i(t)R_i(t)\right)\middle|\ Q_i(t)\right]$$
$$-\mathbb{E}\left[Z(t)\left(\sum_{i=1}^{N}Pg_i(t)-\gamma\right)\middle|\ Z(t)\right], \quad (42)$$

where $B_2>0$ is constant, and by using we obtain the following drift function with reward:

$$\Delta^U(t)=\Delta(t)-V\mathbb{E}\left[\sum_{i=1}^{N}\left(U_i(t)\right)\middle|\left(\mathbf{Q}(\mathbf{t}),Z(t)\right)\right]. \quad (43)$$

By using (42) in the lemma, we obtain an upper bound for (43), as follows:

$$\Delta^U(t)<B_2-V\mathbb{E}\left[\sum_{i=1}^{N}U_i(A_i(t)\right]-\sum_{i=1}^{N}\mathbb{E}\left[Q_i(t)\left(A_i(t)-\mathscr{I}_i(t)R_i(t)\right)|Q_i(t)\right]$$
$$-\mathbb{E}\left[Z(t)\left(\sum_{i=1}^{N}Pg_i(t)-\gamma\right)\middle|\ Z(t)\right]$$
$$=B_2-V\mathbb{E}\left[\sum_{i=1}^{N}U_i(A_i(t)\right]-\mathbb{E}\left[\sum_{i=1}^{N}I_i(t)W_i(t)\middle|\left(\mathbf{Q}(\mathbf{t}),Z(t)\right)\right]$$
$$+\mathbb{E}\left[\sum_{i=1}^{N}Q_iA_i(t)|\mathbf{Q}(\mathbf{t})\right]+\mathbb{E}\left[\sum_{i=1}^{N}Z(t)\gamma|Z(t)\right] \quad (44)$$

By using the bound in the Lemma 3, we obtain further bound for (44), as follows:

$$\Delta^U(t)<B_2-V\mathbb{E}\left[\sum_{i=1}^{N}U_i(A_i(t))\right]-\alpha\mathbb{E}\left[W^*(t)\middle|\left(\mathbf{Q}(\mathbf{t}),Z(t)\right)\right]$$
$$+\mathbb{E}\left[\sum_{i=1}^{N}Q_iA_i(t)|\mathbf{Q}(\mathbf{t})\right]+\mathbb{E}\left[\sum_{i=1}^{N}Z(t)\gamma|Z(t)\right], \quad (45)$$

where $\alpha=(1-M\tau)\left(\frac{N}{M}\left(1-\frac{1}{M}\right)^{N-1}\right)$. The result in (35) suggests that the algorithm at least achieves α portion of minimized drift obtain by centralized algorithm. Again assume that x_i^* denotes optimal traffic arrival rates, which is in the achievable rate region. Then, since αx^* is in the α fraction of the achievable rate region,[5] there must exists a stationary scheduling and rate allocation policy that is independent of queue backlogs and satisfies the following:

$$\mathbb{E}\left[\mathscr{I}_i(t)R_i(t)\right]\geq\alpha{x_i}^*+\varepsilon_3 \text{ and } \sum_{i=1}^{N}\mathbb{E}\left[Pg_i(t)\right]\leq\gamma+\varepsilon_3 \quad (46)$$

Note that as we consider stationary and ergodic policies, long-term averages (46) correspond to expectations of the same variables as in (35). Clearly, any stationary policy in the α fraction of the achievable rate region should satisfy (35). Recall that our proposed policy obtains α fraction of the minimum of the right hand side (RHS) of (35), and hence, any other stationary policy in the α fraction of the achievable rate region has a higher RHS value than the one attained by our policy. In particular, the stationary policy that satisfies (46), and implements aforementioned probabilistic admission control can be used to obtain an upper bound for the RHS of our proposed policy. Inserting (46) into (35), we obtain the following upper bound for our policy:

$$RHS<B_2-\sum_{i=1}^{N}\varepsilon_3\mathbb{E}[Q_i(t)]-\varepsilon_4\mathbb{E}[Z(t)]-V\sum_{i=1}^{N}U_i(\alpha x_i^*). \quad (47)$$

From (47), by taking the time-average over $t=0,1,\ldots,T-1$ and taking the limsup of T, we can prove Theorem 3.

[5] In the previuos section it is defined as $\alpha\Gamma$